ON THE INTERACTION OF POLARIZATION DEPENDENT LOSS WITH OPTICAL FIBER NONLINEARITY

N. Rossi, P. Serena, A. Bononi
Dipartimento di Ingegneria dell'Informazione, Università degli Studi di Parma,
v.le G. Usberti 181/A, 43124 Parma, Italy. Email: rossi_n@tlc.unipr.it

We investigate the interplay of polarization dependent loss with Kerr nonlinearities, namely SPM, XPM and XPolM, in a homogeneous 100G PDM-QPSK or hybrid 100G PDM-QPSK/10G OOK system over a 20x100km NZDSF dispersion-managed link.

1. Introduction

Polarization-division-multiplexed quadrature phase shift keying (PDM-QPSK) is one of the most attractive solutions for 100 Gb/s optical transmissions thanks to the availability of digital signal processing (DSP) units able to cope with linear impairments, like chromatic dispersion (CD) and polarization mode dispersion (PMD). However, DSP cannot completely compensate for polarization dependent loss (PDL), which manifests both as a polarization dependent signal to noise ratio (SNR) as well as a loss of orthogonality between polarization tributaries. The impact of PDL in PDM-QPSK systems operating in the linear regime has been extensively studied in the literature, e.g. [1,2], while only few works investigated the interplay between PDL and the nonlinear Kerr effect [3,4]. These results show a detrimental coupling of PDL with fiber nonlinearities.
Aim of our work is to quantify and explain the interaction between PDL and Kerr effect by decoupling the fiber nonlinearities, namely, self phase modulation (SPM), cross phase modulation (XPM) and cross polarization modulation (XPolM).
We focus on a long haul dispersion managed (DM) link originally designed for "legacy" on-off keying (OOK) channels at 10 Gb/s. Two possible scenarios are considered: "fully upgraded" and "partially upgraded". In the first case all transmitted channels are non-return-to-zero (NRZ) 100 Gb/s PDM-QPSK, giving a homogeneous system. In the second, a single 100 Gb/s PDM-QPSK channel is surrounded by 10 Gb/s NRZ-OOK neighbors, giving a hybrid system.

2. Numerical Setup

We simulated the system depicted in Fig. 1 with the open-source software Optilux [5].

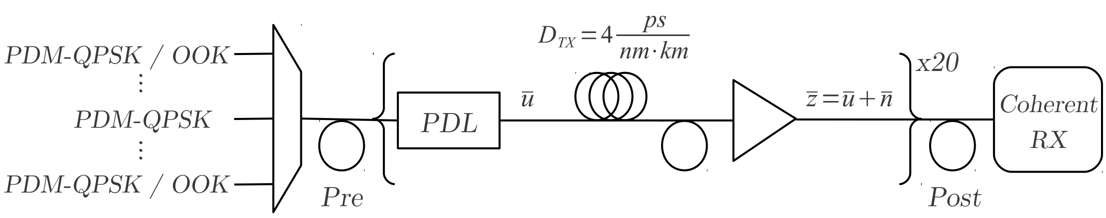

Figure 1: The simulated system with lumped PDL elements along the link.

PDL was described by a lumped element placed before entering the transmission fiber. Its input/output functional relation is expressed as [4]:

$$\begin{bmatrix} u_X^{(i)} \\ u_Y^{(i)} \end{bmatrix} = \begin{bmatrix} \sqrt{1+\Gamma} & 0 \\ 0 & \sqrt{1-\Gamma} \end{bmatrix} \begin{bmatrix} \cos\vartheta_i & \sin\vartheta_i \\ -\sin\vartheta_i & \cos\vartheta_i \end{bmatrix} \begin{bmatrix} \cos\varepsilon_i & j\sin\varepsilon_i \\ j\sin\varepsilon_i & \cos\varepsilon_i \end{bmatrix} \begin{bmatrix} z_X^{(i-1)} \\ z_Y^{(i-1)} \end{bmatrix} \quad (1)$$

where $\overline{z}^{(i-1)} = \overline{u}^{(i-1)} + \overline{n}^{(i-1)}$ is the field at the end of the (i-1)-*th* span, being $\overline{n}$ the

noise added by the amplifier, while subscripts X and Y indicate the two polarizations, respectively. Γ is the normalized PDL coefficient while $(\vartheta_i, \varepsilon_i)$ are the azimuth and ellipticity of the i-*th* PDL element eigenvector. j is the imaginary unit.
The optical link was composed of 20x100 km spans of non-zero dispersion shifted fiber (NZDSF) (attenuation 0.2 dB/km, dispersion 4 ps/nm/km, nonlinear index $\gamma = 1.5$ 1/W/km, no PMD) with residual dispersion per span set to 30 ps/nm. We added a Pre-dispersion of -345 ps/nm before entering the link, while after the link a post-compensating fiber set to zero the overall cumulated dispersion. The propagation within the optical fibers was numerically solved by the split-step Fourier algorithm as a concatenation of linear and nonlinear steps. Each nonlinear step was implemented by activating the nonlinearity of interest, namely SPM, XPM or XPolM, along the same lines of [6].
We assumed flat-gain noisy amplifiers with 7 dB noise figure, thus accounting for the nonlinear signal-noise interaction along the link. The WDM comb consisted of 19 channels, with 50 GHz spacing. The central channel was a 112 Gb/s PDM-QPSK, surrounded by either 112 Gb/s PDM-QPSK channels or by 10 Gb/s OOK channels. In the first case we used for each PDM-QPSK channel 1024 random symbols, in the second 840. The DSP-based receiver performed polarization recovery with a data-aided least squares equalizer with 7 taps and carrier phase estimation through the Viterbi&Viterbi algorithm with 15 taps. The performance was measured in terms of the Q-factor obtained by inverting the bit error rate (BER) of the central channel, estimated from Monte Carlo simulation stopped after counting 100 errors.

3. Simulation Results

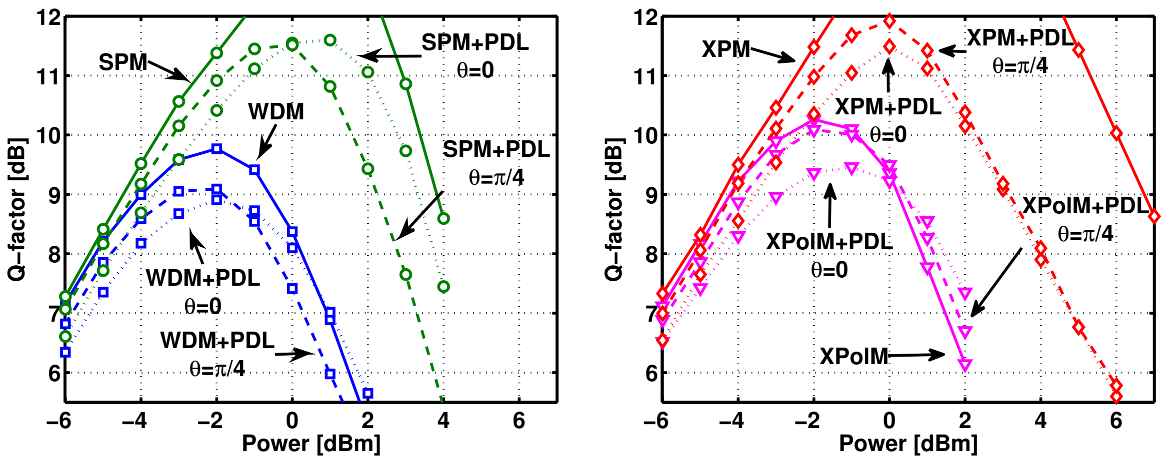

Figure 2: Average performance in the homogeneous 20x100km NZDSF DM link without PDL or with a total PDL of $\rho = 5$ dB, $\varepsilon = 0$. (Left) Propagation of single-channel or WDM. (Right) Propagation with only selected cross-channel impairments.

Fig. 2 shows the average Q-factor vs. signal power using our nonlinearity decoupling method [6] in the homogeneous setup. The performance is averaged over 10 seeds, each corresponding to random carrier states of polarization (SOP) and delay offset of the transmitted channels. Each nonlinear effect has been analyzed separately in three scenarios: i) without PDL (solid lines), ii) with identical PDL sections having $\rho_i = 10\log_{10}\left(\frac{1+\Gamma}{1-\Gamma}\right) = 0.25$ dB and $(\vartheta_i, \varepsilon_i) = (0,0)$ (dotted lines) or iii) $(\vartheta_i, \varepsilon_i) = (\pi/4, 0)$ (dashed lines). Choices ii) and iii) of (ϑ, ε) have been shown to be a worst case of PDL in linear and nonlinear regimes [3,4], respectively. The curve labeled WDM corresponds to the real case including SPM+XPM+XPolM. Even if such pathological cases of all-aligned PDL elements are very unlikely in a real setup, they let us understand the interaction of PDL with Kerr effect in a simple way. We start analyzing the ascending part of the Q-factor curves. Here in all cases the worst PDL is with $(\vartheta,\varepsilon)=(0,0)$ where the polarization dependent SNR degradation induced by PDL is maximum and cannot be compensated by the DSP [3]. The temporal fluctuations of power and SOP induced by PDL have indeed a different impact in the nonlinear regime (descending part of the Q-factor curve): the first affects SPM and XPM within the fiber, the second affects XPolM. The total instantaneous power after the i-*th* PDL element is:

$$P_{out}(t)=\left(\left|z_X^{(i)}\right|^2+\left|z_Y^{(i)}\right|^2\right)+\Gamma\cos 2\vartheta\cos 2\varepsilon\left(\left|z_X^{(i)}\right|^2-\left|z_Y^{(i)}\right|^2\right)$$
$$+\Gamma\cos 2\vartheta\sin 2\varepsilon\left(2\mathrm{I_m}\left\{z_X^{(i)}\left(z_Y^{(i)}\right)^*\right\}\right)+2\Gamma\sin 2\vartheta\left(2\mathrm{R_e}\left\{z_X^{(i)}\left(z_Y^{(i)}\right)^*\right\}\right). \quad (2)$$

For phase modulated signals $\left|z_X^{(i)}\right|^2$ and $\left|z_Y^{(i)}\right|^2$ remain almost constant along propagation in DM systems. Consequently, at $\varepsilon=0$ only the last term in (2) matters, especially when $\vartheta=\pi/4$ [4], making the power fluctuation maximum; however, this ϑ-dependence does not appear for XPM because the transmitted SOPs of the interfering channels are randomly oriented with respect to the central channel, thus removing, on average, the dependence on the absolute reference system of the PDL axes (i.e., on ϑ). The XPM penalty induced by PDL is large because, without PDL, XPM is negligible for constant envelope formats [6].

For XPolM the scenario is different. Here each PDL element acts as a partial polarizer, thus reducing the pattern-induced temporal fluctuations of the SOP, hence reducing XPolM. This can be easily observed from Fig. 3 that depicts over the Poincaré sphere the SOP of a PDM-QPSK signal before and after propagation through a PDL element with $(\vartheta,\varepsilon)=(0,0)$ and $\rho=5$ dB. Fig. 2 (right) indicates that the linear penalty due to PDL is more than compensated by the reduction of XPolM at large powers. Overall, the beneficial impact of PDL over XPolM does not appear on the real WDM curve, an indication that SPM and XPM cannot be neglected when PDL is present. Moreover, the worst case Q-factor of the WDM case shows 1 dB of penalty with respect to the no PDL case at any power, although for different reasons.

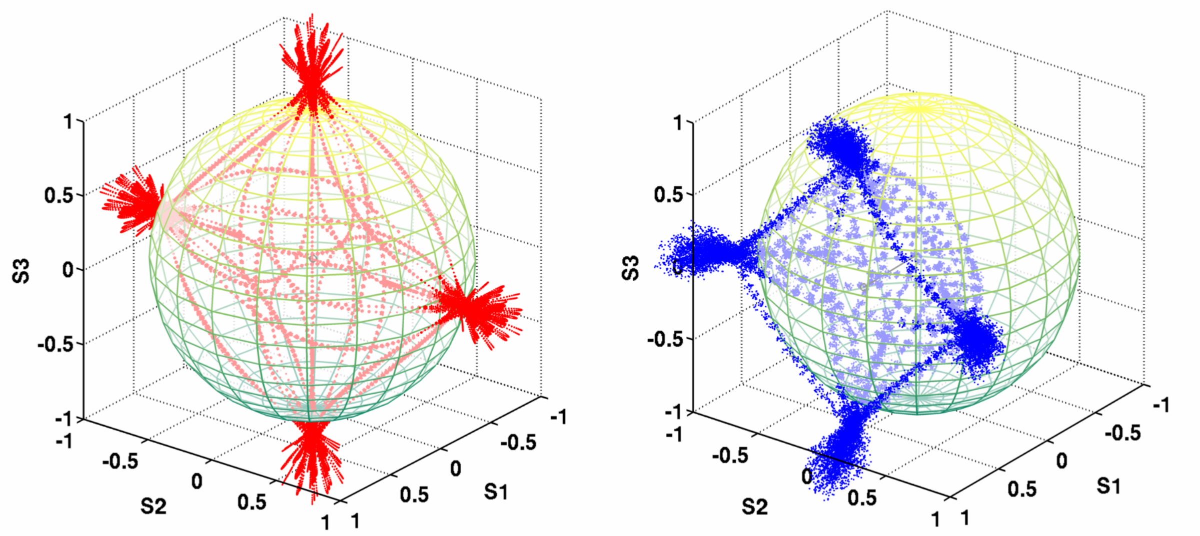

Figure 3: State of Polarization of a PDM-QPSK signal before (Left) and after (Right) propagation through a lumped PDL element with $\rho=5$ dB and $(\vartheta,\varepsilon)=(0,0)$.

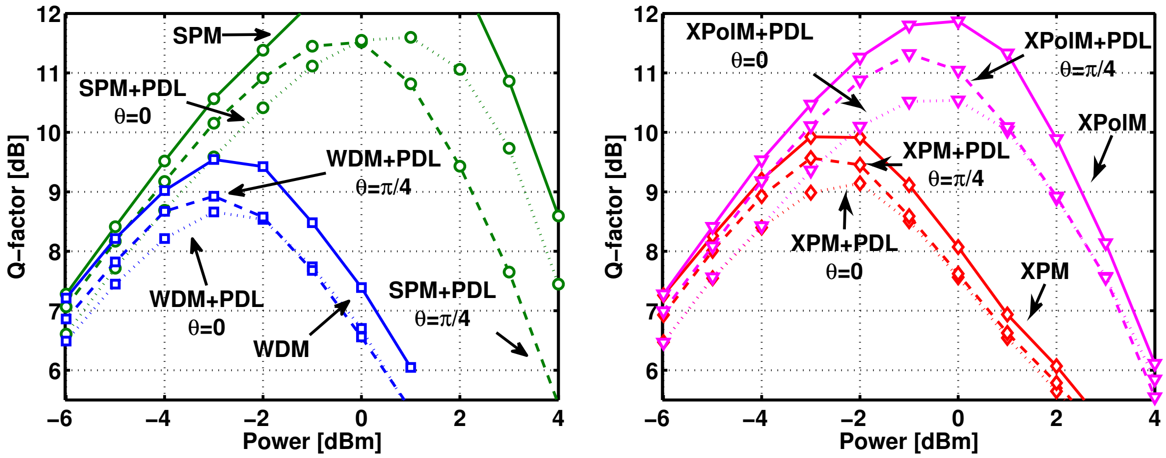

Figure 4: Average performance in the hybrid setup20x100km NZDSF DM link without PDL or with a total PDL of $\rho = 5$ dB, $\varepsilon = 0$. (Left) Propagation of single-channel or WDM. (Right) Propagation with only selected cross-channel impairments switched on.

Moving to the hybrid scenario we replaced PDM-QPSK interfering channels with 10Gb/s OOK having average power locked 4 dBm below that of the central 112 Gb/s PDM-QPSK, in order to have equal back-to-back performance for both modulation formats. Fig. 4 shows the average Q-factor when applying the nonlinear decoupling method. This setup has XPM as the dominant nonlinear distortion because PDM-QPSK suffers the intensity fluctuations of neighboring OOK [7]. Now the second term on the right hand side of (2) causes a ϑ-dependent coupling of XPM with PDL that can be detrimental when $\vartheta = 0$ or beneficial when $\vartheta = \pi/2$. However, the PDL/XPM interaction is in any case masked by the random orientation of the transmitted SOP of the interfering channels. XPolM is now a secondary impairment and does not show improvements with PDL, being the PDL polarizing effect of minor importance with OOK neighbors.

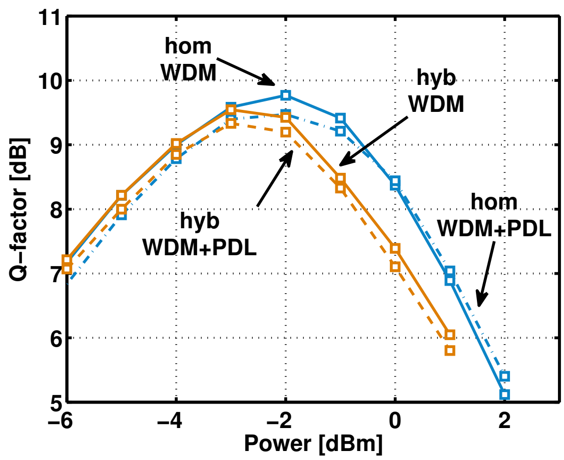

Figure 5: Average performance in both hybrid and homogeneous 20x100km NZDSF DM link for WDM propagation without PDL or with $\rho_{rms} = 2.2$ (PDL elements with random orientation).

When dealing with realistic setups the eigenvectors of PDL elements are randomly oriented, yielding a total cumulated PDL with Maxwellian distribution. The root mean square value (rms) of the distribution is related to ρ_i by $\rho_{rms} = \rho_i \cdot \sqrt{N_{span}}$, being N_{span} the number of spans, yielding in our case $\rho_{rms} = 2.2$ dB. The pathological cases analyzed in Figs. 2 and 4 are very unlikely in real setups with randomly-oriented PDL elements, where a first hint on PDL impact is given by the average Q-factor, depicted in Fig. 5. It can be easily seen that the impact of PDL on average Q-factor is confined within 0.3 dB at any power.

A more detailed description of the impact of PDL is given by the distribution of the Q-factor. To deal correctly with performance distribution it is necessary to separate the input random variables (RVs) in two groups according to their behavior during a BER measurement: i) non-ergodic RVs that do not vary, ii) ergodic RVs that do. The distribution of the Q-factor must account for the randomness of the non-ergodic variables only, while the impact of the ergodic variables must be averaged as in a BER measurement. In our case non-ergodic variables were represented by carrier SOP and PDL orientations $(\vartheta_i, \varepsilon_i)$, while ergodic ones were ASE and symbol patterns. Hence the correct procedure for PMF estimation requires two nested cycles: an inner one on ergodic RVs and an outer one on non-ergodic RVs. This procedure becomes very time consuming when simulating low BER values and calls for simplifications to save on simulation time. A naive procedure is to fix the symbol pattern, i.e. to treat it as a non-ergodic variable, and average the BER over different ASE realizations by loading, after a noiseless propagation, all the equivalent noise at the end of the link, ensuring the same power spectral density. In this case the nonlinear interaction between signal and noise is not taken into account, which has been shown in [7] to be acceptable on average-Q estimation in DM setups for both homogeneous and hybrid scenarios.

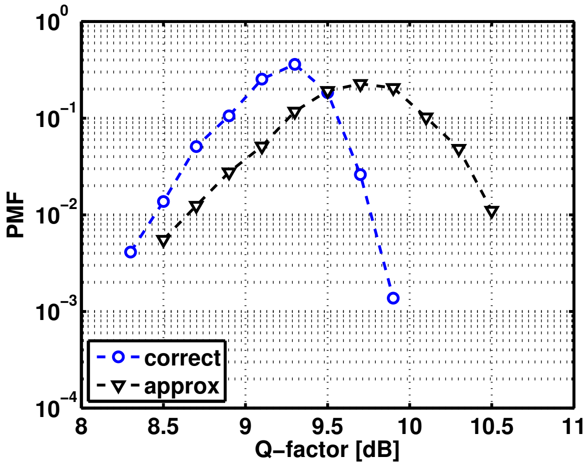

Figure 6: Q-factor Probability Mass Function (PMF) with $\rho_{rms} = 2.2$ (PDL elements with random orientation). 800 random seeds for non-ergodic variables. Homogeneous setup with Power = -1 dBm. (Blue) Correct procedure. (Black) Naive approximated procedure.

Fig. 6 shows the probability mass function (PMF) of the Q-factor in the homogeneous scenario for P = -1 dBm and random PDL elements for a total PDL $\rho_{rms} = 2.2$ dB. It is worth noting that the naive procedure returns not only a 0.4 dB offset on the average Q-factor, in agreement with [7], but also a PMF with doubled variance with respect to the real PMF obtained with the correct procedure. Reasons for the enlarged variance can be searched not only in the missing signal/noise interaction in the naive procedure, but also in the wrong inclusion of symbol patterns into the non-ergodic variables, which increases the occurrence of rare events in both tails of the PMF.

Fig. 7 shows the estimated PMF of the Q-factor in presence and absence of PDL for both homogeneous and hybrid scenarios. Notwithstanding the use of the correct procedure, the real entity of Q-factor fluctuations could be masked by the relative accuracy

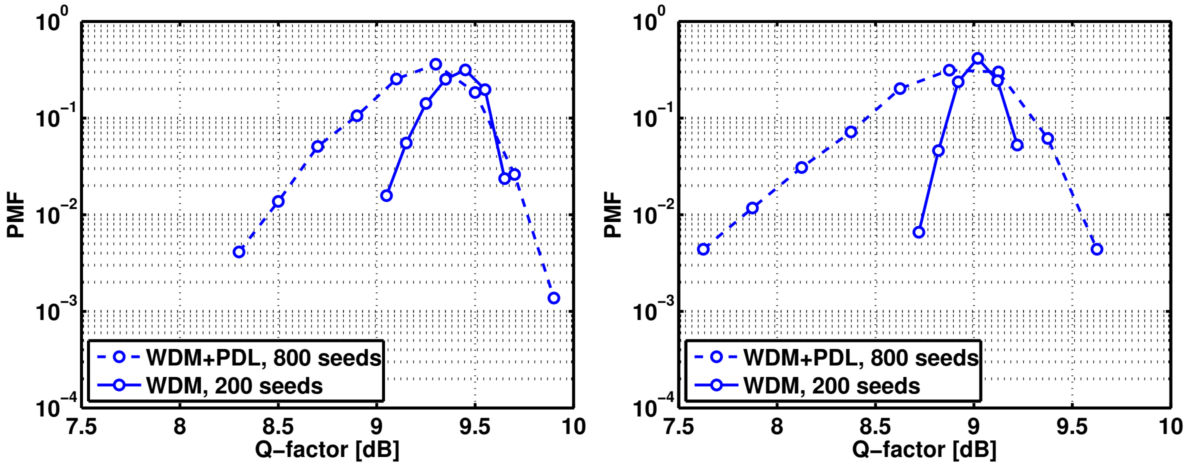

Figure 7: Q-factor Probability Mass Function (PMF) without PDL or with $\rho_{rms} = 2.2$ (PDL elements with random orientation). (Left) Homogeneous setup with Power = -1 dBm, (Right) Hybrid setup with Power = -1.5 dBm.

of Monte Carlo BER estimation in the inner cycle on ergodic RVs, which adds an uncertainty to each Q-factor sample. A PMF is well estimated if the Monte Carlo variance in the ergodic inner cycle is much smaller than the variance of the overall PMF. We verified that in our case inner estimations of Q-factors by counting at least 400 errors in absence of PDL and 100 errors with PDL is enough for an accurate overall PMF estimation. Assuming a forward error correction (FEC) Q-threshold of 8.5 dB, comparing solid with dashed curves we note that with PDL the probability of an outage event, i.e. Q-factor lower than 8.5 dB, is much higher than without PDL, despite similar PMF average values.

4. Conclusions

By decoupling the nonlinear Kerr effects, we showed that PDL has notably different interactions with SPM, XPM and XPolM in dispersion-managed optical systems. We also showed that the presence of realistic random PDL has little impact on average Q-factor but makes a remarkable difference on outage probabilities.

Bibliography

[1] M. Shtaif, “Performance degradation in coherent polarization multiplexed systems as a result of polarization dependent loss”, Opt. Exp., pp. 13918-13932, Sept. 2008.
[2] C. Xie, “Polarization-Dependent Loss Induced Penalties in PDM-QPSK Coherent Optical Communication Systems”, in Proc. OFC 2010, San Diego (USA), paper OWE6.
[3] O. Vassilieva, I. Kim, T. Naito, “Systematic Investigation of Interplay between Nonlinear and Polarization Dependent Loss Effects in Coherent Polarization Multiplexed Systems”, in Proc. ECOC 2010, Torino (Italy), paper P4.08.
[4] Z. Tao, L. Li, T. Hoshida and J. Rasmussen, “Interaction betweem PDL and Intrachannel Nonlinearity in Dual Polarization Systems”, in Proc. OECC 2011, Kaohsiung (Taiwan), paper 6B3_2.
[5] P. Serena et al., *Optilux - an open source of light*, http://optilux.sourceforge.net/.
[6] A. Bononi, P. Serena, N. Rossi, and D. Sperti, “Which is the Dominant Nonlinearity in Long-haul PDM-QPSK Coherent Transmissions?”, in Proc. ECOC 2010, Torino (Italy), paper Th.10.E.1.
[7] A. Bononi, N. Rossi, and P. Serena, “Transmission Limitations due to Fiber Nonlinearity”, in Proc. OFC 2011, Los Angeles (USA), paper OWO7.